ELSEVIER

Biophysical Chemistry 114 (2005) 71–83

Biophysical Chemistry

http://www.elsevier.com/locate/biophyschem

Tryptophan interactions with glycerol/water and trehalose/sucrose cryosolvents: infrared and fluorescence spectroscopy and ab initio calculations

Jennifer L. Dashnau*, Bogumil Zelent, Jane M. Vanderkooi

Johnson Research Foundation, Department of Biochemistry and Biophysics, School of Medicine, University of Pennsylvania, Philadelphia, PA 19104, United States

Received 18 August 2004; received in revised form 13 October 2004; accepted 14 October 2004
Available online 24 November 2004

Abstract

In order to correlate how the solvent affects emission properties of tryptophan, the fluorescence and phosphorescence emission spectra of tryptophan and indole model compounds were compared for solid sugar glass (trehalose/sucrose) matrix and glycerol/water solution and under the same conditions, these matrices were examined by infrared spectroscopy. Temperature was varied from 290 to 12 K. In sugar glass, the fluorescence and phosphorescence emission spectra are constant over this temperature range and the fluorescence remains red shifted; these results are consistent with the static interaction of OH groups with tryptophan in the sugar glass. In sugar glass containing water, the water retains mobility over the entire temperature range as indicated by the HOH infrared bending frequency. The fluorescence of tryptophan in glycerol/water shifts to the blue as temperature decreases and the frequency change of the absorption of the HOH bend mode is larger than in the sugar glass. These results suggest rearrangement of glycerol and water molecules over the entire temperature change. Shifts in the fluorescence emission maximum of indole and tryptophan were relatively larger than shifts for the phosphorescence emission—as expected for the relatively smaller excited triplet state dipole for tryptophan. The fluorescence emission of tryptophan in glycerol/water at low temperature has maxima at 312, 313, and 316 nm at pH 1.4, 7.0, and 10.6, respectively. The spectral shifts are interpreted to be an indication of a charge, or Stark phenomena, effect on the excited state molecule, as supported by ab initio calculations. To check whether the amino acid remains charged over the temperature range, the infrared spectrum of alanine was monitored over the entire range of temperature. The ratio of infrared absorption characteristic of carboxylate/carbonyl was constant in glycerol/water and sugar glass, which indicates that the charge was retained. Tryptophan buried in proteins, namely calcium parvalbumin from cod and aldolase from rabbit, showed temperature profiles of the fluorescence spectra that were largely independent of the solvent (glycerol/water or sugar glass) and temperature whereas the fluorescence and phosphorescence yields were dependent. The results demonstrate how the rich information found in tryptophan luminescence can provide information on the dipolar nature and dynamics of the matrix.

Keywords: Cryosolvents; Sugar glass; Glycerol; Water; Trytophan; Indole; IR; Flourescence; Phosphorescence

1. Introduction

Proteins can possess multiple chromophores: tryptophan, tyrosine, phenylalanine, and cysteine (-S-S-). These residues all contribute to absorption in the UV range [1,2]. However, fluorescence spectra of most tryptophan-containing proteins are dominated by tryptophan due to its high absorption extinction coefficient and efficient fluorescence [3].

The fluorescence of tryptophan is exquisitely sensitive to the environment. Its sensitivity is related to luminescence properties originating from the heteroaromatic indole ring of the residue with an uneven charge distribution around the macrocycle. Upon excitation, there is a very large change in

Abbreviations: NATA, *N*-acetyl-L-tryptophanamide; TS, trehalose/sucrose; ISE, internal Stark effect.

* Corresponding author. Tel.: +1 215 898 8783; fax: +1 215 893 2042.
E-mail address: jdashnau@mail.med.upenn.edu (J.L. Dashnau).

0301-4622/$ - see front matter © 2004 Elsevier B.V. All rights reserved.
doi:10.1016/j.bpc.2004.10.003

the distribution of electrons around the chromophore; electron density is shifted from the pyrrole ring to the benzene portion of the ring [4]. This results in a net dipole moment change of the molecule. The dipole moment of tryptophan in the ground state is 2.13 D [5]. In the excited state, the dipole moment is 5.4 D [6].

Due to large charges on the atoms and the intrinsic polarizability of the indole ring electrons, a charged group nearby a charged portion of the indole macrocycle can influence the electrons of the ring. Since the excited-state molecule has a different distribution than the ground-state molecule, equilibrium arrangement of solvent molecules around the ground state and the excited state is different. The small molecule water is very highly charged; its dipole moment is 2.95 ± 0.2 D [7]. In the presence of the strong electric field produced by indole, water molecules will rearrange position. When water molecules move, they tend to lower the effect of electric fields.

The result of the solvent rearrangement on the fluorescence of tryptophan and its derivatives is a red shift in the emission spectrum [8]. The effect of the solvent on the tryptophan emission is a function of the charges near the group, the rate of relaxation of the dipolar molecules, the nature of the charge distribution of the indole, and the lifetime of the excited state. The interplay between the rate of relaxation of solvent and the spectrum is exemplified by the observation of time-resolved spectral shifts in the spectrum [9].

While most previous studies examined the properties of tryptophan, the condition of the solvents were lesser known [10–16]. In this paper, to see how solvents influence the spectrophysics of tryptophan, we compare the fluorescence and phosphorescence spectra of indole derivatives in two similar matrices that have different dynamic properties. One matrix is glycerol/water (60:40 v/v). This solvent is liquid until about 155 K [17], at which point it undergoes a liquid to glass transition. The second solvent used is trehalose/sucrose glass. These sugars form optically clear glasses at high temperatures (65 °C), which are stable over a large range of temperature [16].

For this study, we compare a wide temperature range (290–12 K), and correlate changes in tryptophan and indole fluorescence and phosphorescence with solvent changes as detected by infrared spectroscopy. One set of experiments relates to the condition of the matrix: What is the nature of the matrix? Do temperature-dependent changes occur in the matrix? The HOH bending mode of water was examined to see whether water rearranges as temperature changes. The infrared spectrum of the carboxyl group was used as a marker for change groups on proteins, and measurements at low and high pH reveal whether amino and carboxyl groups change charge over temperature. The second set of experiments correlates the emission properties of indole with the solvent changes. The parameters of emission maxima for fluorescence and phosphorescence, the fluorescence/phosphorescence yields and phosphorescence lifetimes are measured over a temperature excursion of 290 to 12 K. Three solvent pH conditions were examined to see whether the protonation of tryptophan carboxyl and amino groups affect the emission parameters. Finally, the results are rationalized by examining charge distribution on indole using quantum calculation at the HF/6-31G* level of theory. It is shown that the charge distribution depends upon the protonation of the amino group and the dielectric of the solvent.

2. Materials and methods

2.1. Materials

Water was deionized and glass distilled. Glycerol 99%, α-D-glucopyranosyl-α-D-glucopyranoside (D(+) trehalose), α-D-glucopyranosyl-β-D-fructofuranoside (sucrose), L-Alanine (Sigma Grade), *N*-acetyl-L-tryptophanamide (NATA), 3-methylindole 99% and aldolase from rabbit were supplied by Sigma (St. Louis, MO). Fluka BioChemika provided L-tryptophan. Calcium parvalbumin was prepared from frozen codfish [18].

2.2. Methods

2.2.1. Sugar glass preparation

Protein or tryptophan compounds in trehalose/sucrose (TS) glass were prepared as described previously [19]. Trehalose (300 mg) and sucrose (300 mg) were dissolved in 500 μL distilled water to form TS stock solution. Samples were prepared as solutions in 10 mM potassium phosphate buffer, pH 7.0, with the optical density of tryptophan at 280 nm between 1 and 2 OD units. For 3-methylindole, saturated samples in phosphate buffer had an absorbance of less than 1 OD units; therefore, solubility of the sample was increased with addition of 5–10% ethanol. The sugar glass was prepared by adding 100 μL of TS stock solution to 400 μL of sample solution. Following this step, the sample was placed on a 25-mm quartz plate of 2-mm thickness (Esco Products, Oak Ridge, NJ) and allowed to solidify on a VWR Scientific Products Heat Block at 65 °C overnight. The resulting sugar glasses were hard to the touch and optically clear. Final A_{280} measurements were made with the dried TS glass to insure absorbance between 0.5 and 1 OD units for fluorescence measurements using front-face geometry. For IR measurements, 10 μL of the stock sugar solution and 16 μL of 1 M L-alanine in D_2O were dissolved in 300 μL of D_2O. After adjustment of pD at room temperature to 3.0 using 1 M of DCl or to pD 10.0 using NaOD, the sample solution was pipetted to cover a 25 mm round CaF_2 disk (Janos Technology, Townshend, VT), which was placed on the heat block at 65 °C for approximately 2 h until the sample was dry.

2.2.2. Cryo-solution preparation

Protein or tryptophan compounds in glycerol/water were prepared by first creating 10 mM potassium

phosphate buffer solutions as described above. Visible absorption spectra were measured using a Hitachi Perkin-Elmer U-3000 spectrophotometer (Newtown, PA) and absorbance was adjusted to between 1 and 2 OD units at 1-cm path length. Glycerol was then added to the samples to obtain a 60% glycerol/water cryo-solution. Samples were applied between circular quartz plates separated with a 200 μm Teflon spacer. For IR measurements, 6 μL of 1 M L-alanine in D_2O were diluted in 2 μL of D_2O plus 12 μL of glycerol-D_8. After adjustment of pD to 3.0 or 10.0, the sample solution (20 μL) was placed between two round CaF_2 plates with a 6-μm Teflon spacer. For glycerol/water IR samples, 20 μL glycerol/water (60:40) was placed between two round CaF_2 plates with a 6 μm Teflon spacer. Trehalose/sucrose IR samples were prepared by dissolving 20 μL trehalose/sucrose stock solution in 380 μL water on a CaF_2 plate. The samples were then allowed to dry fully to form TS dry or partially to form TS wet (sticky).

2.2.3. Spectroscopy

Emission spectra and phosphorescence lifetime of the studied compounds were measured with a Fluorolog-3-21 Jobin-Yvon Spex Instrument SA (Edison, NJ) equipped with a 450-W Xenon lamp for excitation and a cooled R2658P Hamamatsu photomultiplier tube for detection. Front-face geometry was used for all measurements. A 278- or 280-nm excitation wavelength was used to observe fluorescence and phosphorescence emission in the 290–500-nm range. Slit width was set to provide a band-pass from 2 to 5 nm for excitation and 2 nm for emission. High-resolution spectra were measured at lowest temperature with 1-nm slit for emission taken every 0.5 nm. Correction for the photo-response of the photomultiplier tube was made to all spectral measurements through the instrument software. Phosphorescence decay was measured using Time-Based Acquisition Mode setting of the DataMax software. The emission monochromator was set at the maximum peak of phosphorescence.

Sample temperature for temperature-dependent emission measurements was regulated using an APD closed cycle Helitran cryostat (Advanced Research Systems, Allentown, PA). A chamber was constructed to alleviate strain on windows due to contraction at low temperature. For fluorescence/phosphorescence measurements, the outer windows of the compartment were made of quartz and the inner windows were made of sapphire. Temperature was measured and controlled using a silicon diode near the sample connected to a Model 9650 temperature controller (Scientific Instruments, Palm Beach, FL). Temperature-dependent measurements were performed from high to low temperature at 10-K increments.

Infrared absorption spectra were obtained with a Bruker IFS 66 Fourier transform IR spectrophotometer (Bruker, Brookline, MA). The sample compartment was purged with nitrogen to reduce the contribution from water vapor, and light levels were monitored using an HgCdTe (MCT) detector. The spectral resolution was 2 cm^{-1}. All spectra were taken in the transmission mode and transformed to absorption. The spectra were smoothed using a Savitsky–Golay smoothing algorithm. The same Helitran cryostat described above was used for IR measurements, except in this case windows of CaF_2 were used on the outer cryostat. The inner cryostat windows were 2-mm thick and were made of ZnSe (Janos Technology).

2.2.4. Spectra analysis

SigmaPlot 2001 Version 7.101 (SPSS) was used to analyze fluorescence data. Fluorescence peaks were fitted with Weibull function to determine intensity and peak maximum position. PeakFit Version 4.11 (SYSTAT) was used to analyze phosphorescence data from 400 to 500 nm. Phosphorescence peaks were fitted with Gaussian function following smoothing with the Savitzky–Golay algorithm to determine intensity and peak maximum position for all components. Peak maximum position for fluorescence and phosphorescence (0,0 transition) were plotted versus wavelength and further fitted with sigmoidal curve function when appropriate to determine position at high temperature and low temperature as well as the midpoint of the shift. Additionally, phosphorescence maximum intensity was plotted as a fraction of fluorescence maximum intensity across a range of temperature.

Infrared spectra were analyzed for their components using the PeakFit Program following Savitsky–Golay smoothing described above. A Gaussian function in the form:

$$a_0 \exp\left[-0.5\left(\frac{x-a_1}{a_2}\right)^2\right]$$

where a_0, a_1 and a_2 denote amplitude, maximal position and widths, respectively, was used for deconvolution of peaks.

2.2.5. Protein analysis

The program GETAREA was used to determine the percent of tryptophan exposure to external solvent environment [20] based on PDB files 1EX5 [21] and 1BU3 [22] for aldolase and calcium parvalbumin, respectively.

2.2.6. Molecular modeling

Tryptophan was constructed and Cartesian coordinates were obtained using CS Chem3D Pro Version 3.5.1 (CambridgeSoft Corporation, Cambridge, MA). The coordinates were then transferred to GAUSSIAN98 [23] for geometry optimization at the HF/6-31G* level of theory. The optimized geometries for L-tryptophan under neutral, positive and negative charge were used for further calculation. The charges on atoms were calculated and transferred to DELPHI for dielectric reaction field energy calculations. The calculations were performed under solvent dielectric of 80 and 2 with all other values left at the program default. MOLDEN [24] was used for electric field visualization. When constructing electric field gradients, the rings of tryptophan were placed in the grid plane with atom C7 in

the center of the grid. All electric field gradients were based on the true electrostatic potential function in MOLDEN.

3. Results

3.1. Infrared characterization of solvent

3.1.1. Studies of water in trehalose/sucrose glass and glycerol/water

Infrared spectra were taken over a range of temperature under different solvent conditions—glycerol/water, TS wet and TS dry. Fig. 1 shows the IR spectra for water in TS dry (A), TS wet (B) and glycerol (C) from 1200 to 1800 cm^{-1}. TS dry contains little water in comparison to TS wet and glycerol solvent conditions. TS wet produces a more prominent peak than TS dry between 1600 and 1700 cm^{-1}. This peak, identified as arising from HOH bending mode, is centered at ~1650 cm^{-1}. The absorption bands of the water (HOH) bending regions were examined for position shifting with temperature. In TS glass, the absorption maximum of this peak shifts little (~9 cm^{-1}) in the range of the temperature change. In contrast, the HOH bending shift in glycerol is >20 cm^{-1}; the HOH bending band shifts from 1652 cm^{-1} at room temperature to 1676 cm^{-1} at low temperature (12 K).

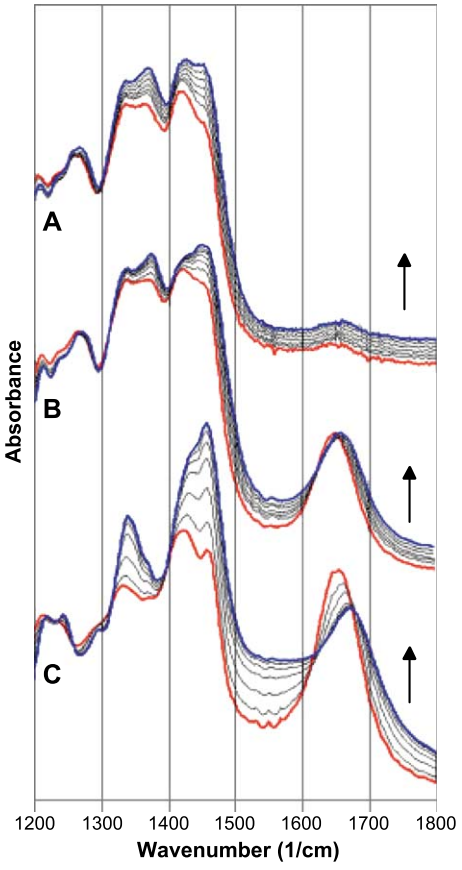

Fig. 1. IR absorption spectra of TS dry (A), TS wet (B), and 60% glycerol/water (C) from 290 K to 12 K. Arrows indicate direction of decreasing temperature.

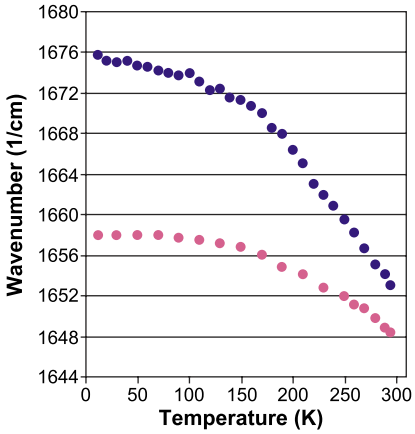

Fig. 2. Temperature dependence of the HOH bending maximum position of water in glycerol (dark circles) and TS wet (light squares) (see Fig. 1).

The shift of the HOH bending mode is further depicted in Fig. 2, which shows the wave number versus temperature for the HOH bending band in glycerol and TS wet. The shift is greater for HOH in glycerol, and at the lowest temperature the frequency of the bending mode absorption is higher for HOH in glycerol than in TS sugar glass.

3.1.2. Studies of protonation in trehalose/sucrose glass and in glycerol/water

Infrared spectroscopy can be used to monitor the ionization state of the carboxyl group [25]. The limited solubility of tryptophan hinders its use in IR, but alanine was employed as a model amino acid. The absorption of L-alanine in D8-glycerol/D_2O is shown in Fig. 3A. The peak at 1610 cm^{-1} is attributed to the stretch mode of the carboxylate group and the peak at 1720 cm^{-1} is the stretch of the carbonyl from the protonated carboxyl group. The pD is chosen so that there is approximately equal molar ratio of each at room temperature (the difference in absorption arises from different extinction coefficients). The ratio of intensities does not change with temperature. A similar profile is seen for L-alanine in trehalose/sucrose glass (Fig. 3B). In Fig. 3C, the spectrum of L-alanine at pD 10 is shown. In this case, the carboxylate absorption is measured and the pD is chosen such that there is approximately equal contribution from alanine where the amino group is protonated and deprotonated (i.e., neutral). The peak at 1570 cm^{-1} arises from the neutral form. The ratios of intensities remain approximately the same, indicating that the protonation does not change over the temperature range. The carboxylate frequency shifts lower as temperature is lowered—consistent with increased hydrogen bonding to solvent [26]. The change in frequency as a function of temperature is documented in Fig. 4. These data show that in both solvents the ionization of carboxylate and amino groups is retained over the temperature range.

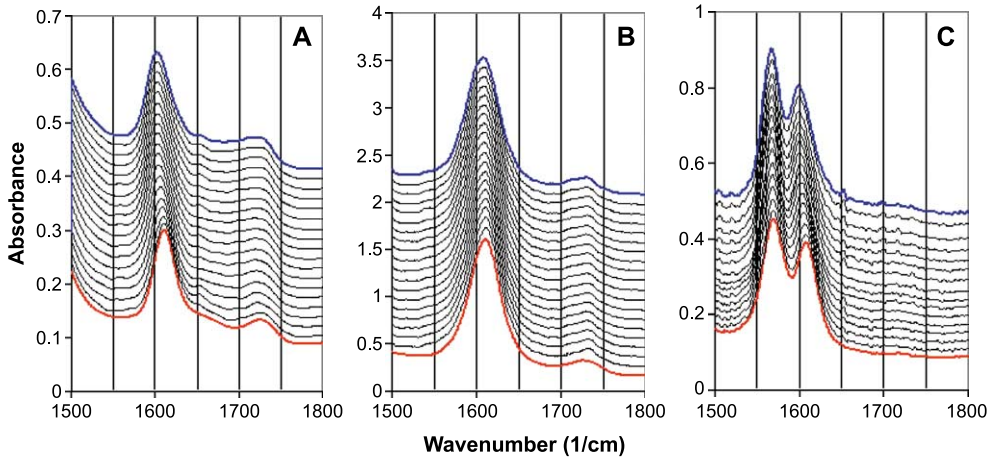

Fig. 3. IR absorption spectra of the carboxylate and carbonyl stretching region of L-Ala in D_8-glycerol/D_2O (60:40, v/v) pD 3.0 (A); trehalose/sucrose glass (1:1 molar ratio prepared at 65 °C), pD 3.0 (B); D_8-glycerol/D_2O (60:40, v/v), pD 10.0 (C). The temperature was varied from 295 K (bottom-most spectra) to 12 K (upper-most spectra). ν^{a}_{OCO} is seen at 1610 cm^{-1} (A, B) and 1570 cm^{-1} (C). ν_{CO} is seen at 1730 cm^{-1} (A, B) and 1600 cm^{-1} (C).

3.2. Emission spectra

Emission spectra of tryptophan and indole derivatives in the two solvents were taken over a range of temperatures and pH conditions. Representative spectra are given in this section. Table 1 summarizes the fluorescence and phosphorescence peak emission positions.

3.2.1. Indole emission in solid and fluid protic environments

Fig. 5 shows the emission spectra of NATA from high temperature (290 K) to low temperature (12 K) in dry TS glass and glycerol/water. The emission from 290 to 390 nm arises from fluorescence, and the peaks from 400 to 500 nm come from phosphorescence. When in the same solvents, NATA and 3-methylindole (spectra not shown) exhibit similar emission profiles. In dry TS glass (Part A of Fig. 5), the fluorescence spectral profile retains its shape and little shifting occurs in λ_{max} over the temperature excursion. This has been previously reported [19]. However, in glycerol/water (Part B of Fig. 5) and in wet TS glass (not shown), fluorescence parameters change drastically with temperature. At high temperature, the spectrum is broader, of lower intensity, and more red shifted than that seen at low temperature. We note that the fluorescence spectrum at low temperature shows significant changes in profile as compared to the spectrum at high temperature. The striking difference between the two solvents is an indication of dissimilarity in dynamics, which we discuss later.

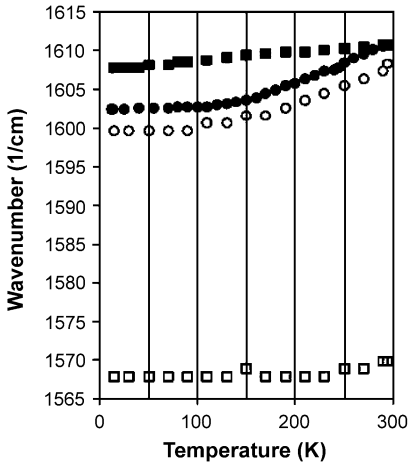

Fig. 4. Temperature dependence of the frequency peak positions of the IR υ^{a}_{OCO} absorption band. L-Ala in TS glass at pD 3.0 (filled squares), L-Ala in D_2O-D_8-glycerol at pD 3.0 (filled circles), and at pD 10.0 (open circles and open squares).

3.2.2. Tryptophan emission in protein environments

The effect of protein environment was determined by examining temperature-dependent fluorescence and phosphorescence for proteins in which tryptophan is buried within the protein. Two proteins with buried tryptophan—calcium parvalbumin and aldolase—are ideal models. The single tryptophan in calcium parvalbumin located at residue 102 is completely buried with calculated solvent exposure of 0%. The three tryptophan residues of aldolase monomer—W147, W295 and W313—have solvent exposure of 0%, 0.3% and 1.6%, respectively. Both calcium parvalbumin and aldolase represent examples of cases where tryptophan is highly buried within the protein. The effect of buried tryptophan residues on phosphorescence for a number of proteins is discussed in review articles [3,24].

Fig. 6 shows emission spectra for calcium parvalbumin. Spectra for aldolase are not shown. In dry TS glass (Part A of Fig. 6), fluorescence spectra for tryptophan in both proteins are similar; there is only a small increase in intensity and no observable shifting occurs in λ_{max} from high to low temperature. In glycerol/water (Part B of Fig. 6), fluorescence at high temperature is less defined and of lower intensity than that seen at low temperature. In the case of the proteins, the fluorescence peaks do not shift in either solvent but the

Table 1
Fluorescence and phosphorescence (0,0 transition) peak position of indole compounds as a function of temperature

Compound	Solvent	pH	Fluorescence			Phosphorescence		
			Min (~12 K)	Max (290 K)	Inflection pt (K)	Min (~12 K)	Max (290 K)	Inflection pt (K)
L-tryptophan	60% glycerol/H_2O	1.4	312.1	340.1	225.9	405.2	408.8	173.8
L-tryptophan	60% glycerol/H_2O	7.0	313.3	344.6	220.6	405.2	413.2	180.4
L-tryptophan	60% glycerol/H_2O	10.6	316.3	351.8	216.2	407.8	413.5	170.7
L-tryptophan	TS film	7.0	320.7			412.2		
L-tryptophan	TS film	10.6	326.9			409.9		
3-methylindole	glycerol/H_2O, EtOH, (60/32/8%)	7.0	322.9	353.0	224.0	415.2	418.3	170.2
3-methylindole	TS film	7.0	327.1			415.6		
NATA	60% glycerol/H_2O	7.0	315.8	347.6	219.8	406.4	413.5	175.1
NATA	TS film	7.0	321.9			409.5		
Calcium parvalbumin	60% glycerol/H_2O	7.0	315.2			407.6		
Calcium parvalbumin	TS film	7.0	313.4			408.5		
Aldolase	60% glycerol/H_2O	7.0	313.1			411.2		
Aldolase	TS film	7.0	316.6			411.0		

For S-shaped curves, minimum, maximum, shift amount and shift midpoint are listed. For linear plots, only the position at minimum temperature is listed.

intensity is markedly temperature dependent in the fluid glycerol/water solvent.

3.2.3. Spectral properties of exposed and buried indoles in solvents

The spectra presented in Figs. 5 and 6 contain information on both fluorescence and phosphorescence, and we now compare the temperature dependence. Fig. 7A,B shows the effect of tryptophan solvent exposure on temperature-dependent fluorescence maximum change in TS glass and glycerol/water, respectively. Fluorescence maximum is constant across temperature for tryptophan residues that are buried in proteins in both TS glass and glycerol/water. Peak position remains between 313 and 316 nm for calcium parvalbumin and aldolase in both conditions. For exposed indole, as in NATA and 3-methylindole, solvent composition

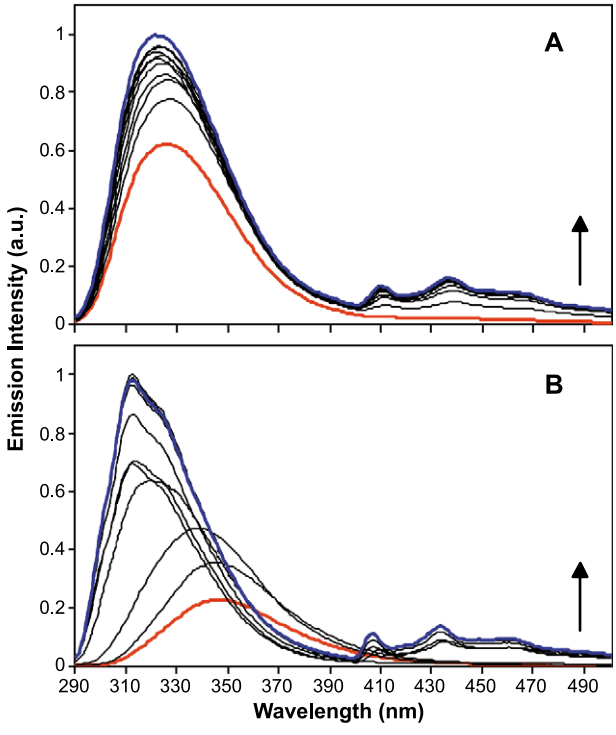

Fig. 5. Fluorescence/phosphorescence emission spectra of NATA at 290 K and 12 K in TS film (A) and 60% glycerol/water (B). Also shown are data for 30-K increments. Arrows indicate direction of decreasing temperature.

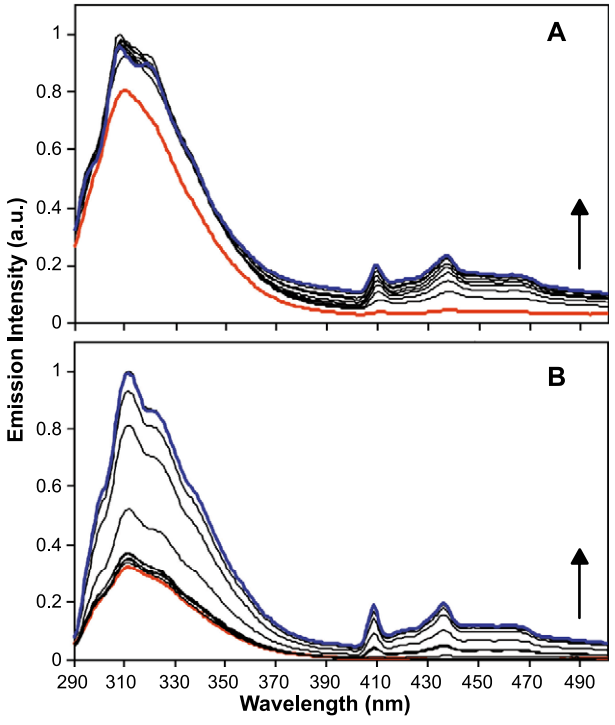

Fig. 6. Fluorescence/phosphorescence emission spectra of calcium parvalbumin at 290 K and 12 K in TS film (A) and 60% glycerol/water (B). Also shown are data for 30-K increments. Arrows indicate direction of decreasing temperature.

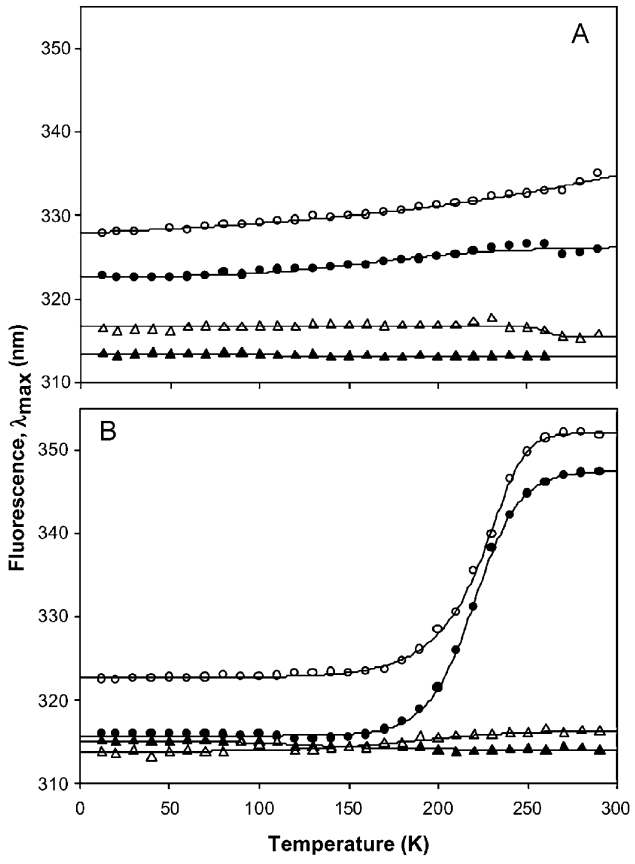

Fig. 7. Effect of protein environment on temperature dependence of fluorescence maximum position of NATA (filled circles), 3-methylindole (open circles), calcium parvalbumin (filled triangles), and aldolase (open triangles) in TS film (A) and 60% glycerol/water (B).

affects fluorescence peak position. In TS glass, λ_{max} changes in an approximately linear fashion over temperature; the peak becomes slightly red shifted at higher temperatures. In glycerol/water, λ_{max} exhibits a larger red shift with a sigmoidal trend. Shift in fluorescence maximum position from low to high temperature is approximately 10-fold greater for exposed indole in glycerol/water than in TS glass. Numerical data are summarized in Table 1.

The effect of protein environment, or degree of solvent exposure, on change in phosphorescence maximum position for protein and compounds in TS glass and glycerol/water is shown in Fig. 8A,B. Phosphorescence exhibits trends similar to those seen for fluorescence. Buried tryptophan residues show constant λ_{max} in both TS glass and glycerol/water. Exposed indole exhibits phosphorescence with constant peak position in TS glass but shifting position in glycerol/water.

The ratio of phosphorescence intensity to fluorescence intensity varies for proteins and reference compounds as shown in Fig. 9A,B (Table 2). This result is an indication that the ratio of the intersystem crossing rate constant to the single state depopulation rate constants as well as the triplet state depopulation rate constant are affected by solvent. To test this, phosphorescence lifetimes were measured and are presented in Table 3. For buried tryptophan residues, solvent composition plays less a role in determining phosphorescence lifetime than when the indole ring is exposed [27–30].

3.2.4. Emission of tryptophan in glycerol/water under different protonation states

The effect of solvent pH on tryptophan spectral properties was determined through measurement in solvents with three pH values: 1.4, 7.0 and 10.6. High and low pH values were selected to be at least one pH unit below the carboxy-terminus pK_a (2.4) and one unit above the amino-terminus pK_a (9.4) of free tryptophan [31].

The fluorescence and phosphorescence of indole will shift according to the local electric field around the chromophore [32]. To impose a field, the charge on part of the molecule that is not conjugated to the ring was charged by changing the pH. Fig. 10 compares the normalized emission spectra of tryptophan in glycerol/water solutions of varying pH at low and high temperature. The fluorescence maximum positions for tryptophan change significantly with solvent pH at high temperature; there is a 12-nm red shift in λ_{max} from pH 1.4 to pH 10.6. In contrast, at low temperature, the fluorescence maximum positions are

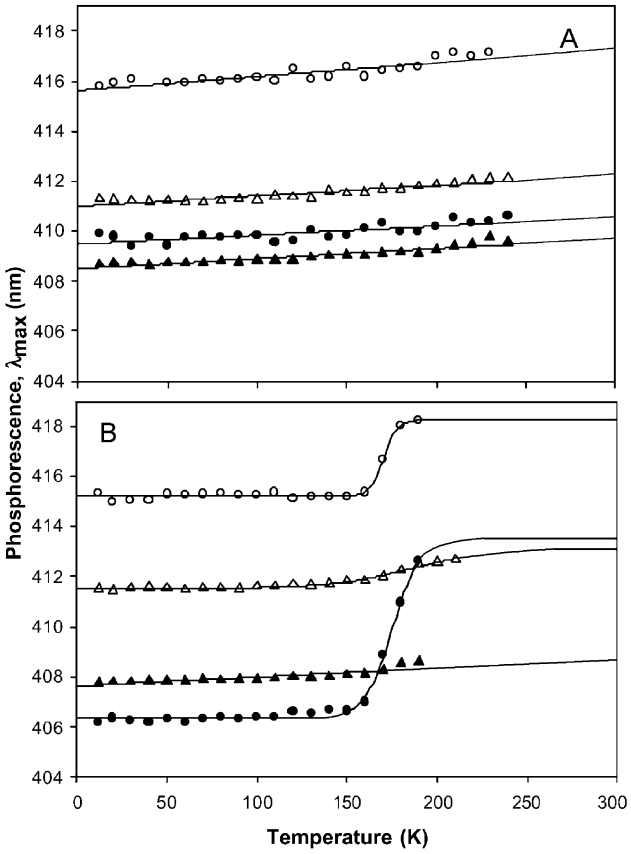

Fig. 8. Effect of protein environment on temperature dependence of phosphorescence maximum position of NATA (filled circles), 3-methylindole (open circles), calcium parvalbumin (filled triangles), and aldolase (open triangles) in TS film (A) and 60% glycerol/water (B).

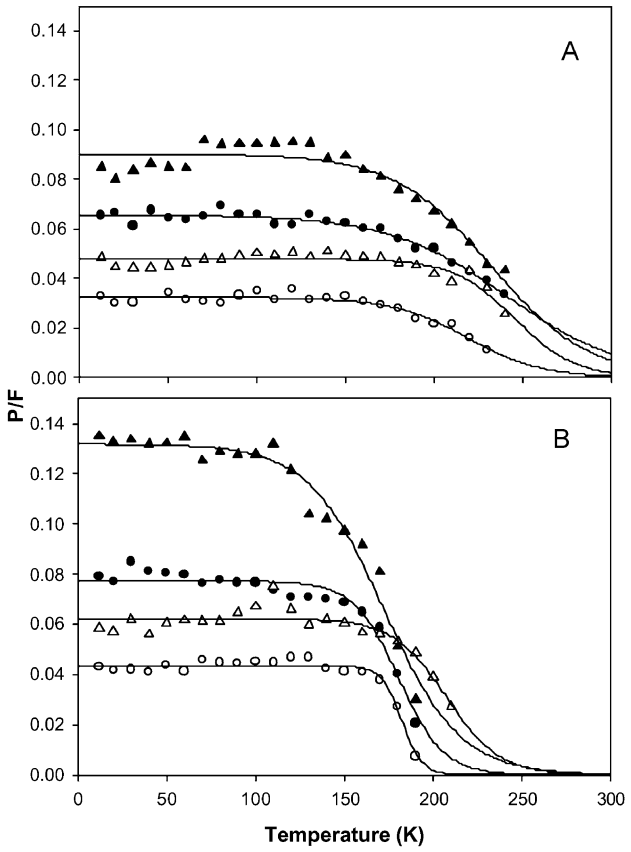

Fig. 9. Effect of protein environment on temperature dependence of phosphorescence intensity as a fraction of fluorescence intensity of NATA (filled circles), 3-methylindole (open circles), calcium parvalbumin (filled triangles), and aldolase (open triangles) in TS film (A) and 60% glycerol/water (B).

only slightly affected by solvent pH; the shift in λ_{max} from pH 1.4 to pH 10.6 is only 4 nm. The shifts are further illustrated in Fig. 11B, which shows the effect of solvent pH on temperature dependence of fluorescence λ_{max} for L-tryptophan under various pH conditions of the glycerol/water solvent. At high temperature, tryptophan fluorescence is red shifted to 351 nm at pH 10.6 and blue shifted to 340 nm at pH 1.4 when compared with pH 7.0 conditions (344 nm). Change in solvent pH also has an affect on the magnitude of fluorescence maxima shift across the temperature range. As pH increases, the amount of shifting from high to low temperature increases; λ_{max} shifts 28 nm under low pH and 36 nm under high pH. However, the temperature at which the midpoint of fluorescence maximum shift occurs is similar across pH—with values from 220 to 225 K—markedly above the glass transition for solvent (155 K). In contrast, the fluorescence λ_{max} for L-tryptophan does not change greatly with temperature; values remain nearly constant at 321 and 328 nm for pH 7.0 and pH 10.6, respectively. For numerical data, see Table 1.

Fig. 12 shows the effect of solvent pH on temperature dependent change of phosphorescence λ_{max}. In glycerol/water, the phosphorescence maximum position of tryptophan is dependent upon temperature. At high temperature, the peak position of tryptophan phosphorescence in solvent pH 10.6 is similar to that in neutral pH solvent. In contrast, at low temperature, phosphorescence at pH 1.4 approaches values similar to pH 7. For all pH conditions, the shift midpoint is around 175 K. However, the amount of shifting varies; phosphorescence of neutral tryptophan undergoes a larger shift with temperature than either of the charged molecules. In TS glass, the peak position is not as greatly affected by temperature. Tryptophan phosphorescence exhibits peaks around 412 and 410 nm across the tested temperature range for solvent pH 7.0 and 10.6, respectively. We were unable to get results for tryptophan in dry TS glass at pH 1.4 due to reactions of the sugars at this pH.

Fig. 13 shows the phosphorescence intensity as a fraction of fluorescence intensity across temperature for tryptophan in different pH solvents. The P/F ratio for all glycerol/water solvent pH experimental conditions mirrors the ratio observed for the tryptophan control condition in glycerol/water pH 7.0. However, in TS glass, differences exist in the ratio for the charged and neutral conditions. While the ratio values for the two conditions fit expected values, the shift point of neutral tryptophan in TS glass is uncharacteristically low compared to other exposed indoles. Numerical data are summarized in Tables 1 and 2.

Phosphorescence lifetime increases slightly with increased pH as seen in Table 3. Average lifetime increases from 5.13 s at pH 1.4 to 5.50 s at pH 7.0 and 5.68 s at pH 10.6.

3.3. Molecular modeling

Fig. 14 shows the electric field gradients of L-tryptophan when the molecule is overall positively charged (A), neutral (B) and negatively charged (C). When the molecule is neutral, a negative electric field surrounds the oxygen of the

Table 2
Phosphorescence intensity of indole compounds as a fraction of fluorescence intensity across temperature

Compound	Solvent	pH	Max	Shift pt (K)
L-tryptophan	60% glycerol/H_2O	1.4	0.071	178.2
L-tryptophan	60% glycerol/H_2O	7.0	0.075	179.0
L-tryptophan	60% glycerol/H_2O	10.6	0.072	183.0
L-tryptophan	TS film	7.0	0.046	170.3
L-tryptophan	TS film	10.6	0.054	223.2
3-methylindole	glycerol/H_2O/EtOH (60/32/8%)	7.0	0.043	182.1
3-methylindole	TS film	7.0	0.032	218.7
NATA	60% glycerol/H_2O	7.0	0.077	180.3
NATA	TS film	7.0	0.066	241.3
Calcium parvalbumin	60% glycerol/H_2O	7.0	0.132	172.1
Calcium parvalbumin	TS film	7.0	0.090	232.2
Aldolase	60% glycerol/H_2O	7.0	0.062	207.0
Aldolase	TS film	7.0	0.048	245.6

For curves fitting sigmoidal function, maximum P/F at low temperature and shift midpoint are listed.

Table 3
Phosphorescence lifetime of indole compounds at low temperature

Protein	Solvent	pH	Temperature (K)	Peak (nm)	Average (s)	SD
L-tryptophan	60% glycerol/H_2O	1.4	15	432	5.13	0.067
L-tryptophan	60% glycerol/H_2O	7.0	12	431	5.50	0.000
L-tryptophan	60% glycerol/H_2O	10.6	12	434	5.68	0.042
L-tryptophan	TS film	7.0	12	412 439	3.16	0.086
3-methylindole	glycerol/H_2O/EtOH (60/32/8%)	7.0	12	442	5.54	0.25
3-methylindole	TS film	7.0	11	441	3.63	0.17
NATA	60% glycerol/H_2O	7.0	12	433	5.40	0.29
NATA	TS film	7.0	11	432	4.09	0.082
Calcium parvalbumin	60% glycerol/H_2O	7.0	12	435	5.23	0.11
Calcium parvalbumin	TS film	7.0	12	436	4.36	0.025
Aldolase	60% glycerol/H_2O	7.0	12	411 438	3.11	0.32
Aldolase	TS film	7.0	12	411 438	3.53	0.31

carboxyl group-stemming from the negatively charged oxygen of this group. As seen by the number and spacing of the contours, this negative electric field is relatively weak in peak intensity compared to the positively charged field surrounding the rest of the molecule. As the molecule becomes positively charged, the localized negative electric field disappears entirely while the positive electric field remains relatively unchanged. In contrast, as the neutral molecule becomes negatively charged, the negative electric field intensifies—peaking at three locations corresponding to the two carboxyl oxygens and the unpaired electrons of the amine group. The location of this charged field is mainly at the pyrrole end of the indole ring—a positioning that has a large affect on spectroscopic characteristics of the molecule.

The electrostatic contribution to free energy of solvation (kcal/mol) for tryptophan in solvent with dielectric 80 and 2 is presented in Table 4. In solvents with high dielectric, such as those with high water content, the charged molecules have a more negative free energy of solvation (−106.45 and −93.90 kcal/mol, for the positive and negative molecules, respectively) than the neutral molecule (−21.48 kcal/mol). In solvents with low dielectric constant, as would be expected for those containing a high percentage of organic molecules, the difference is less noticeable: -3.38×10^{-2} for the neutral molecule versus -6.72×10^{-2} and -4.07×10^{-2} for the positive and negative molecules, respectively.

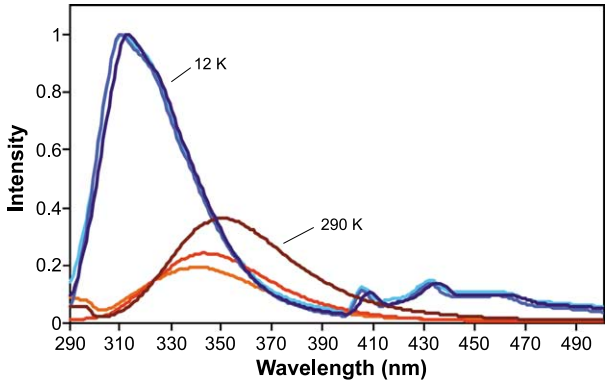

Fig. 10. Normalized emission spectra of L-tryptophan in 60% glycerol/water at pH 1.4 (light), pH 7.0 (medium) and pH 10.6 (dark) at high temperature and low temperature.

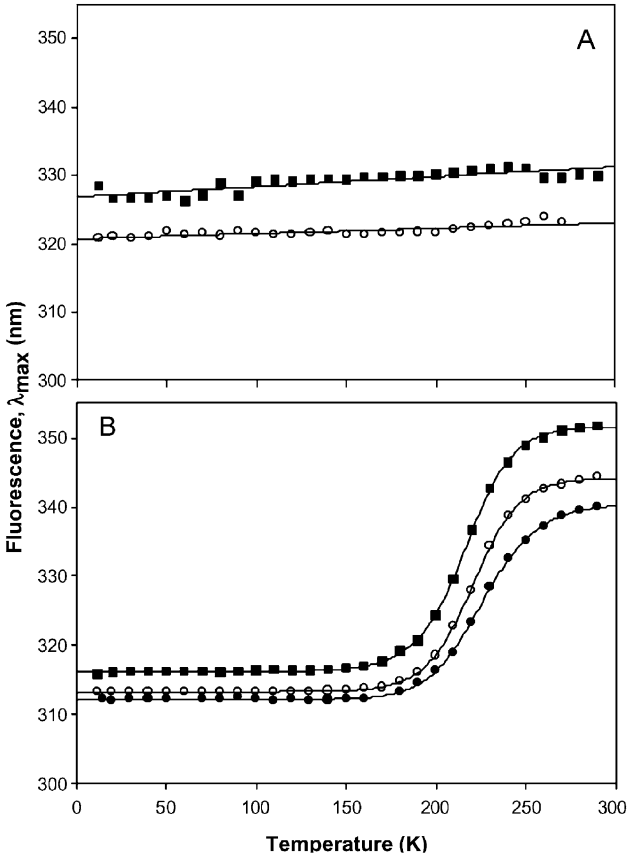

Fig. 11. Effect of solvent pH on temperature dependence of fluorescence maximum position of L-tryptophan in TS glass (A) and 60% glycerol/water (B) at pH 10.6 (filled squares), pH 7 (open circles) and pH 1.4 (filled circles).

4. Discussion

4.1. Microenvironment rearrangement as a function of temperature

Dipolar interactions and hydrogen bonding are the predominant forces that influence water structure. As temperature decreases, hydrogen-bonding strength gets stronger, and the frequency of the HOH bend goes higher [33]. The relationship between frequency and hydrogen bonding is demonstrated by comparing the bending frequency for water in gas and liquid; these values are 1594.7 and 1648 cm^{-1}, respectively [34]. In looking at our data, we note that at room temperature the water bending frequency in TS film has the same value as liquid water, whereas the bending frequency for water in glycerol/water solutions has a slightly higher value (Fig. 2). A higher value, indicating ordering of water, is also reported for water in ethanol solutions [35]. As temperature decreases, in both solid trehalose or in glycerol, the frequency of the HOH bending band increases, but the shift is larger for water in glycerol/water (Fig. 2). The net result is that at low temperature, the hydrogen-bonding characteristic of water in the trehalose/sucrose glass more resembles that of liquid water than does the water in glycerol/water glass.

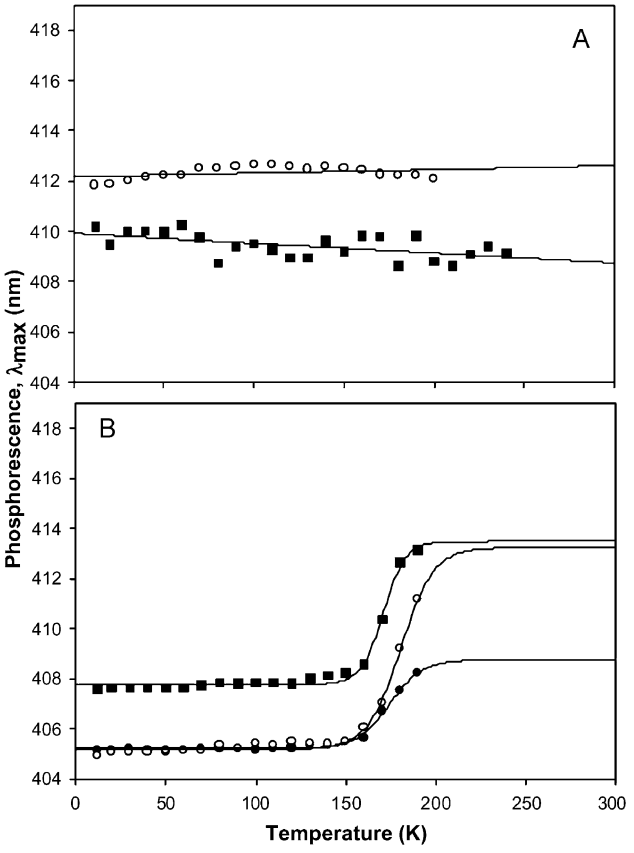

Fig. 12. Effect of solvent pH on temperature dependence of phosphorescence maximum position at 0,0 transition of L-tryptophan in TS glass (A) and 60% glycerol/water (B) at pH 10.6 (filled squares), pH 7 (open circles) and pH 1.4 (filled circles).

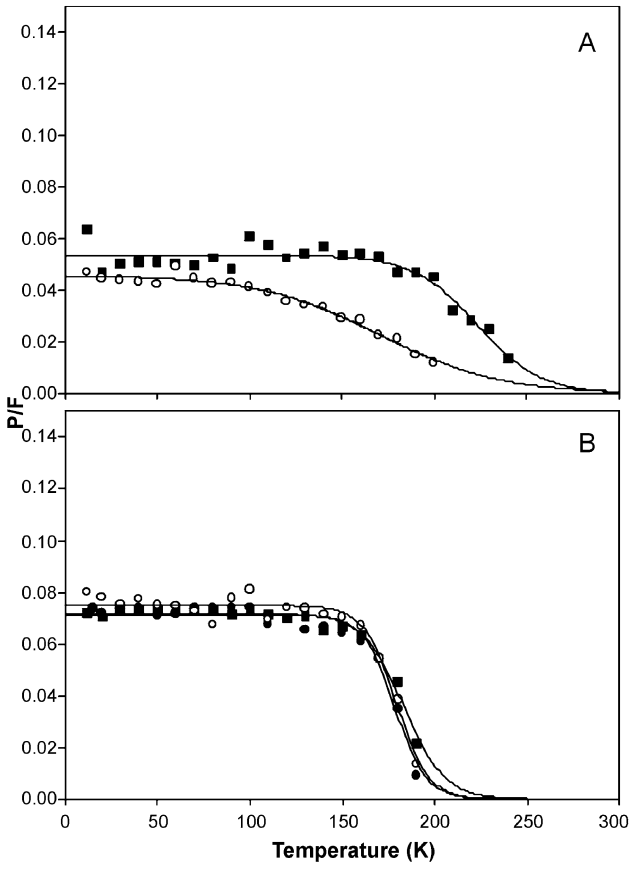

Fig. 13. Effect of solvent pH on temperature dependence of phosphorescence intensity as a fraction of fluorescence intensity of L-tryptophan in TS glass (A) and 60% glycerol/water (B) at pH 10.6 (filled squares), pH 7 (open circles) and pH 1.4 (filled circles).

A possible explanation for the decreased restriction of water movement in TS is that in lower concentrations, such as those seen in TS, water molecules lack the ability to become structured with other water molecules at low temperature due to their isolation in the TS glass matrix. In glycerol/water, where the water concentration is higher, more water–water interactions are able to form. The tunneling of hydrogen of one water molecule to form a bond with adjacent water would occur even at low temperature. In dry TS glass, there is little change in the IR spectra over the temperature excursion (Fig. 1), indicating without water the sugar molecules do not have the ability to rearrange as temperature decreases.

Preservation of the sugar environment in dry TS is demonstrated further through the effect of its rearrangement on indole spectra discussed in the next section. Before moving to that discussion, one should note that when studying samples at low temperature, one must also be concerned that protonation of groups change. In both solvents, the protonation of amino and carboxyl groups were retained over the temperature range (Fig. 3). In glycerol/water, the peak of the symmetric COO^- stretch

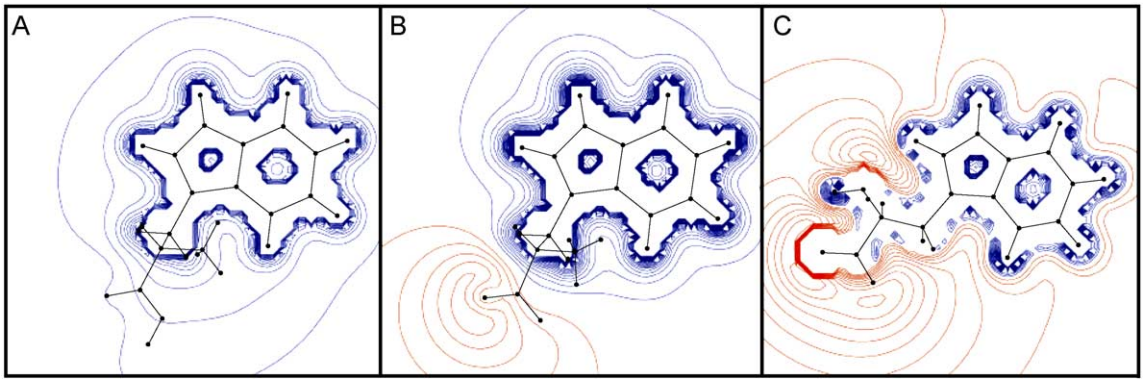

Fig. 14. Electric field gradient of L-tryptophan, charge +1 (A), charge 0 (B), charge-1 (C). Red contours indicate negative charge and blue contours indicate positive charge. Contour values are in increments of 0.0125.

shifts with temperature (Fig. 4). The shift to lower frequency means that the asymmetric stretch mode was stabilized by hydrogen bonding. This stabilization was not enough to significantly change the p*K* of the group, however.

4.2. Spectral characteristics are dependent on microenvironment rearrangement

Solvent-exposed tryptophan can realize hydrogen-bonding contributions from several water molecules in the surrounding environment, thereby resulting in greater electron transfer from the indole pyrrole ring to benzene ring [8]. Therefore, solvent-exposed tryptophans are generally more likely to exhibit larger red shifts than buried tryptophans. As noted above in this study, both NATA and 3-methylindole exhibit large red shifts of close to 30 nm with change in temperature (Fig. 7B). In glycerol/water, this shift occurs as temperature is decreased from ~250 to 180 K—temperatures prior to the glass transition (155 K). These results suggest that as solvent viscosity increases due to decrease in temperature, the ability of solvent molecules to reorient themselves in response to solute excitation decreases. At temperatures below the glass transition, fluorescence maximum does not change. However, the λ_{max} positions of NATA and 3-methylindole at temperatures less than 155 K are lower than those observed for the same compounds in TS film.

In dry TS film, NATA and 3-methylindole do not exhibit large fluorescence maximum shifts with change in temperature. Instead, the λ_{max} positions for these compounds remain constant around 323 and 327 nm for NATA and 3-methylindole, respectively (Fig. 7A). These results suggest that any interactions formed between solvent and solute in solid, stable TS matrix at room temperature are preserved at low temperature. When wet TS film is used, the spectra do show shifts. The water in wet TS film rearranges with temperature, as indicated by its HOH bending frequency (Fig. 2).

The fluorescence spectra profiles for NATA and 3-methylindole in glycerol/water and TS glass (Fig. 5) support these conclusions. In glycerol/water at room temperature, the fluorescence profile of exposed indole is broad and unstructured—similar in shape to that seen when in TS glass. However, as temperature is lowered below 200 K, the spectra become more defined and cease to shift. This result can be explained in terms of OH group ability to interact with indole. Glycerol/water has a larger concentration of OH groups than TS glass; a 60:40 (v/v) mixture contains an approximate 1:3 molar ratio of glycerol (three OH groups) to water. Assuming a random arrangement of solvent around the solute, the OH groups in glycerol/water should also be able to interact with the indole chromophore. We surmise that as temperature decreases the liquid solvent rearranges to lowest energy conformation and hydrogen bonding between the OH groups of glycerol and water increases—making glycerol/water OH groups less available for interaction with the indole rings. In TS film, where OH groups are not as readily available for interaction, the fluorescence profile remains unstructured and stationary throughout the temperature excursion.

For calcium parvalbumin and aldolase (Fig. 6), examples of tryptophan residues in buried environments, no shift is exhibited in either glycerol/water or TS glass. This result correlates with the findings of Vivian and Callis [8]; buried tryptophan is less influenced by solvent polarity and interactions. This provides an additional argument that it is mobile water producing the shift. We point out also that there is a slight increase in profile structure definition. Similar results are seen for the 0,0 transition of phosphorescence. This effect does not seem to be correlated with water content.

The rigidity of TS glass also influences phosphorescence lifetime and at room temperature phosphorescence can be seen for chromophores in films [36–38]. At low temperature, phosphorescence lifetime was lower for indole in the exposed compounds relative to the buried compounds (Table 3). These results appear to contradict findings that lifetime is solely dependent upon solvent viscosity [39]. A possible explanation for this discrepancy lies in the structure of the indole ring. It is possible that the rigid TS glass distorts the indole of the exposed compounds studied—

leading to a ~1.5–2 s decrease in phosphorescence lifetime. In proteins where the tryptophan residues are buried, the decrease is less drastic (calcium parvalbumin) or an increase is observed (aldolase).

4.3. Spectra are influenced by internal Stark effect

The fluorescence results seen in this study can further be explained in terms of internal Stark effect, or shifts related to the electric field imposed by the amino and carboxyl groups of tryptophan. Quantum mechanical studies have predicted red shifts (λ_{max} shifts to longer wavelengths) to be related to positive charges near the benzene ring or negative charges near the pyrrole ring of indole. Protonation of the amine group of tryptophan, as seen when solvent pH is lowered to pH 1.4, leads to creation of a positive electric field near the pyrrole ring of the residue. This field induces the blue shift in fluorescence maximum seen at higher temperatures (Fig. 11). When solvent pH is raised to pH 10.6, the negative charges of the carboxyl and amino groups produce negative electric fields localized near the tryptophan pyrrole ring. The negative field in this location creates the red shift in fluorescence maximum (Fig. 11). These conclusions are further supported by molecular modeling (Fig. 14). The electrostatic field gradients for the neutral and charged molecules display positioning of the negative fields relative to the pyrrole ring.

Phosphorescence exhibits trends similar to that of fluorescence. However, the neutral tryptophan molecule undergoes a larger shift in phosphorescence maximum than either of the charged molecules (Fig. 12). The neutral molecules move from a maximum position characteristic of the deprotonated form at high temperature to a position characteristic of the protonated form at low temperature. This result may be explained by the zwitterionic state of the carboxyl and amino groups of tryptophan at pH 7.0, which has its own dipole. This dipole could possibly disturb water molecule rearrangement around the tryptophan dipole at high temperature—thus explaining the higher energy state of tryptophan phosphorescence at pH 7.0 and high temperature. The results can also be explained in terms of free energy of solvation (Table 4). The charged molecules have a more negative free energy of solvation than the neutral molecule. Therefore, less energy is required for solvent rearrangement surrounding the charged molecules. Fluorescence spectra likely do not exhibit the same characteristics due to differences in emission lifetime in relation to time needed for water rearrangement; phosphorescence exists on the order of milliseconds to seconds whereas fluorescence lifetime lasts for nanoseconds.

For both fluorescence and phosphorescence, the effect of pH is retained across the entire temperature range; that is, the deprotonated state (net charge −1) consistently shifts spectra to the red and the protonated state (net charge +1) consistently shifts spectra to the blue in relation to the net neutral state. Retention of the pH effect is an indication that water molecules do not rearrange enough to neutralize the charge effect.

Table 4
Electrostatic contribution to free energy of solvation (kcal/mol) for tryptophan in solvent with dielectric 80 and 2

Compound, charge	Electrostatic contribution to free energy of solvation (kcal/mol)	
	Solvent dielectric 80	Solvent dielectric 2
L-tryptophan, 0 charge	−21.48	-3.38×10^{-2}
L-tryptophan, +1 charge	−106.45	-6.72×10^{-2}
L-tryptophan, −1 charge	−93.90	-4.07×10^{-2}

5. Summary

Tryptophan luminescence provides a wealth of information related to solvent matrix dynamics. Studies of tryptophan fluorescence and phosphorescence emission over a range of temperature (290 to 12 K) in glycerol/water and trehalose/sucrose matrix illustrate the ability of solvent molecules in fluid matrices, such as glycerol/water prior to the glass transition (155 K), to rearrange. As temperature is decreased below the glass transition, the liquid solvent rearranges to lowest energy conformation causing hydrogen-bonding interactions between the OH groups of glycerol and water increases—making glycerol/water OH groups less available for interaction with the indole rings. In more rigid media (trehalose/sucrose), fluorescence and phosphorescence emission spectra are constant over temperature—demonstrating the static interaction of OH groups with tryptophan. In both glycerol/water and TS glass, water retains the ability to rearrange and relax at even the lowest temperature. Internal Stark effect is also observed for the indole chromophore of tryptophan when in varying degrees of protonation. The pH effect seen is retained across all temperatures—an indication that water does not rearrange enough to neutralized the charge effect. Tryptophan residues buried in proteins (calcium parvalbumin and aldolase) exhibit profiles of fluorescence spectra independent of solvent and temperature effects; that is, these tryptophan residues do not show spectral changes.

Acknowledgements

This work was supported by the National Institutes of Health grant PO1 GM 48130. Additionally, the authors would like to thank Dr. Manoranjan Panda for discussions regarding quantum mechanical modeling.

References

[1] C.N. Pace, F. Vajdos, L. Fee, G. Grimsley, T. Gray, How to measure and predict the molar absorption coefficient of a protein, Protein Sci. 4 (1995) 2411–2423.

[2] H. Mach, D.B. Volkin, C.J. Burke, C.R. Middaugh, Ultraviolet absorption spectroscopy, in: B.A. Shirley (Ed.), Methods in Molecular Biology, vol. 40, Humana Press, Totowa, NJ, 1995, pp. 91–114.
[3] J.W. Longworth, Excited states of proteins and nucleic acids, in: R.F. Steiner, I. Weinryb (Eds.), Excited states of proteins and nucleic acids, Plenum Press, New York, 1971, pp. 319–484 Chapter 6.
[4] P.R. Callis, Molecular orbital theory of the ^1L_a and ^1L_b states of indole, J. Chem. Phys. 95 (1991) 4230–4240.
[5] A.L. McClellan, Tables of Experimental Dipole Moments, Freeman, London, 1963.
[6] H. Lami, N. Glasser, Indole's solvatochromism revisited, J. Chem. Phys. 84 (1986) 597–604.
[7] A.V. Gubskaya, P.G. Kusalik, The total molecular dipole moment for liquid water, J. Chem. Phys. 117 (2002) 5290–5302.
[8] J.T. Vivian, P.R. Callis, Mechanisms of tryptophan fluorescence shifts in proteins, Biophys. J. 80 (2001) 2093–2109.
[9] D. Toptygin, L. Brand, Spectrally- and time-resolved fluorescence emission of indole during solvent relaxation: a quantitative model, Chem. Phys. Lett. 322 (2000) 496–502.
[10] R.P. DeToma, J.H. Easter, L.J. Brand, Dynamic interactions of fluorescence probes with the solvent environment, J. Am. Chem. Soc. 98 (1976) 5001–5007.
[11] J.R. Lakowicz, H. Cherek, Dipolar relaxation in proteins on the nanosecond timescale observed by wavelength-resolved phase fluorometry of tryptophan fluorescence, J. Biol. Chem. 255 (1980) 831–834.
[12] A.P. Demchenko, K. Gryczynski, Z. Gryczynski, W. Wiczk, H. Malak, M. Fishman, Intramolecular dynamics in the environment of the single tryptophan residue in staphylococcal nuclease, Biophys. Chem. 48 (1993) 39–48.
[13] M. Gonnelli, G.B. Strambini, Glycerol effects on protein flexibility: a tryptophan phosphorescence study, Biophys. J. 65 (1993) 131–137.
[14] R.G. Bryant, The dynamics of water–protein interactions, Annu. Rev. Biophys. Biomol. Struct. 25 (1996) 29–53.
[15] J.T. Vivian, P.R. Callis, Mechanisms of tryptophan fluorescence shifts in proteins, Biophys. J. 80 (2001) 2093–2109.
[16] W.W. Wright, C.J. Baez, J.M. Vanderkooi, Mixed trehalose/sucrose glasses used for protein incorporation as studied by infrared and optical spectroscopy, Anal. Biochem. 307 (2002) 167–172.
[17] I. Yannas, Vitrification temperature of water, Science 160 (1968) 298–299.
[18] K. Sudhakar, C.M. Philips, S.A. Williams, J.M. Vanderkooi, Dynamics of parvalbumin studied by fluorescence emission and triplet absorption spectroscopy of tryptophan, Biochemistry 34 (1993) 1355–1363.
[19] W.W. Wright, G.T. Guffanti, J.M. Vanderkooi, Protein in sugar glass and in glycerol/water as examined by infrared spectroscopy and by the fluorescence and phosphorescence of tryptophan, Biophys. J. 85 (2003) 1980–1995.
[20] R. Fraczkiewicz, W. Braun, Exact and efficient analytical calculation of the accessible surface areas and their gradients for macromolecules, J. Comp. Chem. 19 (1998) 319–333.
[21] A. Maurady, A. Zdanov, D. De Moissac, D. Beaudry, J. Sygusch, A conserved glutamate residue exhibits multifunctional catalytic roles in D-fructose-1,6-bisphosphate aldolases, J. Biol. Chem. 277 (2002) 9474.
[22] S.P. Revett, G. King, J. Shabanowitz, D.F. Hunt, K.L. Hartman, T.M. Laue, D.J. Nelson, Characterization of a helix-loop-helix (EF Hand) motif of silver hake parvalbumin isoform B, Protein Sci. (1997) 2397–2407.
[23] M.J. Frisch, G.W. Trucks, H.B. Schlegel, G.E. Scuseria, M.A. Robb, J.R. Cheeseman, V.G. Zakrzewski, J.A. Montgomery Jr., R.E. Stratmann, J.C. Burant, S. Dapprich, J.M. Millam, A.D. Daniels, K.N. Kudin, M.C. Strain, O. Farkas, J. Tomasi, V. Barone, M. Cossi, R. Cammi, B. Mennucci, C. Pomelli, C. Adamo, S. Clifford, J. Ochterski, G.A. Petersson, P.Y. Ayala, Q. Cui, K. Morokuma, P. Salvador, J.J. Dannenberg, D.K. Malick, A.D. Rabuck, K. Raghavachari, J.B. Foresman, J. Cioslowski, J.V. Ortiz, A.G. Baboul, B.B. Stefanov, G. Liu, A. Liashenko, P. Piskorz, I. Komaromi, R. Gomperts, R.L. Martin, D.J. Fox, T. Keith, M.A. Al-Laham, C.Y. Peng, A. Nanayakkara, M. Challacombe, P.M.W. Gill, B. Johnson, W. Chen, M.W. Wong, J.L. Andres, C. Gonzalez, M. Head-Gordon, E.S. Replogle, J.A. Pople, Gaussian 98, Gaussian, Pittsburgh, PA, 1998.
[24] G. Schaftenaar, J.H. Noordik, J. Comput.-Aided Mol. 14 (2000) 123.
[25] W.W. Wright, J.M. Vanderkooi, Use of IR absorption of the carboxyl group of amino acids and their metabolites to determine p*K*s, to study proteins, and to monitor enzymatic activity, Biospectroscopy 3 (1997) 457–467.
[26] E.S. Manas, Z. Getahu, W.W. Wright, W.F. DeGrado, J.M. Vanderkooi, Infrared spectra of amide groups in α-helical proteins: evidence for hydrogen bonding between helices and water, J. Am. Chem. Soc. 122 (2000) 9883–9890.
[27] S. Papp, J. Vanderkooi, Tryptophan phosphorescece at room temperature as a tool to study protein structure and dynamics, Photochem. Photobiol. 49 (1989) 775–784.
[28] N.K. Shah, R.D. Ludescher, Phosphorescence probes of the glassy state in amorphous sucrose, Biotechnol. Prog. 11 (1995) 540–544.
[29] E. Gabellieri, G.B. Strambini, Structural perturbations of azurin deposited on solid matrices as revealed by Trp phosphorescence, Biophys. J. 80 (2001) 2431–2438.
[30] C.J. Fischer, A. Gafni, D.G. Steel, J.A. Schauerte, The triplet-state lifetime of indole in aqueous and viscous environments: significance to the interpretation of room temperature phosphorescence in proteins, J. Am. Chem. Soc. 124 (2002) 10359–10366.
[31] R.H. Garrett, C.M. Grisham, Biochemistry, Saunders College Publishing, Philadelphia, 1995.
[32] D.W. Pierce, S.G. Boxer, Stark effect spectroscopy of tryptophan, Biophys. J. 68 (1995) 1583–1591.
[33] G.A. Jeffrey, An Introduction of Hydrogen Bonding, Oxford University Press, New York, 1997.
[34] T. Shimanouchi, in: P.J. Linstrom, W.G. Mallard (Eds.), NIST Chemistry WebBook, 2001, NIST Gaithersburg, MD, http://webbook.nist.gov.
[35] K. Mizuno, Y. Miyashita, Y. Shindo, H. Ogawa, NMR and FT-IR studies of hydrogen bonds in ethanol–water mixtures, J. Phys. Chem. 99 (1995) 3225–3228.
[36] C.P. McCaul, R.D. Ludescher, Room temperature phosphorescence from tryptophan and halogenated tryptophan analogs in amorphous sucrose, Photochem. Photobiol. 70 (1999) 166–171.
[37] N.K. Shah, R.D. Ludescher, Phosphorescence probes of the glassy state in amorphous sucrose, Biotechnol. Prog. 11 (1995) 540–544.
[38] J.S. Wang, R.J. Hurtubise, Solid–matrix luminescence from trace organic compounds in glasses prepared from sugars, Appl. Spectrosc. 50 (1996) 53–58.
[39] G.B. Strambini, M. Gonnelli, The indole nucleus triplet-state lifetime and its dependence on solvent microviscosity, Chem. Phys. Lett. 115 (1985) 196–200.